Post-wildfire debris flow in the Northwestern Italian Alps: description and numerical analysis of the June 2018 Bussoleno event

Landslides
DOI 10.1007/s10346-025-02605-9
Received: 12 March 2025
Accepted: 29 July 2025

G. La Porta · A. Leonardi · S. La Ferlita · M. Pirulli

Post-wildfire debris flow in the Northwestern Italian Alps: description and numerical analysis of the June 2018 Bussoleno event

Abstract On June 7, 2018, a mud-debris flow occurred in the *Comba delle Foglie* basin, Susa Valley, Northwestern Italy. The event followed an unusually wet winter and spring with high cumulative rainfall, though no intense rainfall was recorded immediately prior to the flow. Approximately 20,000 m^3 of sediments and woody debris were transported to an urbanized alluvial fan, causing severe damage, including the destruction of two residential buildings and widespread flooding. Key predisposing factors include extensive wildfires in Autumn 2017, which are atypical for this region characterized by an alpine climate. Following the event, significant mitigation measures were implemented. This study presents an analysis of the event, integrating data on fire damage, rainfall distribution, flow runout, and deposit thickness from post-event surveys. A numerical back-analysis of the flow dynamics is conducted using two approaches to define the triggering area. The *simplified triggering* approach applies a method frequently used in the literature, simulating the runout of a concentrated mass to evaluate the flow's rheology. Two rheological laws are tested by comparing simulated flow depths and path with field data. The *susceptibility-based triggering* approach incorporates a preliminary susceptibility analysis, integrating fire severity mapping and literature findings to account for wildfire-induced impacts on soil stability. A comparison of the simulations shows that the susceptibility-based analysis better reproduces the flow path, enhancing back-analysis accuracy. However, the simplified approach remains a reliable tool for the case study. Finally, the effectiveness of the implemented mitigation measures is assessed through numerical simulations, providing insights into the settlement's potential response to future debris-flow events.

Keywords Mudflow · Debris flow · Wildfire · Numerical modeling · Triggering and runout · Depth-averaged model

Introduction

Mountainous areas worldwide are subjected to mud- and debris-flow hazards if rainfall occurs at least occasionally (Hungr and Jakob 2005), and if a source of sediment supply is available. This can be an elevated sediment deposit that is naturally replenished by erosion of exposed bedrock, or by the occurrence of a landslide (McCoy et al. 2010; Ma et al. 2018). Additionally, sediments can become quickly available when vegetated land is scorched by wildfire (Moody et al. 2013). Wildfires can significantly alter both the mechanical and hydrological properties of soils, increasing susceptibility to shallow landslides and debris flows. The thermal degradation of vegetation, particularly root systems, leads to a substantial reduction in soil strength by diminishing the apparent cohesion typically provided by roots (Secci et al. 2014; Peduto et al. 2022; Lei et al. 2022). Concurrently, the thermal impact can induce changes in soil structure, including the formation of hydrophobic layers and reduced hydraulic conductivity. These alterations influence the slope's hydrological response by limiting infiltration and promoting rapid surface runoff during rainfall events (Debano 2000; Doerr et al. 2004; Ebel and Moody 2020). As a result, post-fire debris flows can be expected during common rainstorms (Esposito et al. 2023). Additionally, burned areas have been observed to generate 2.7 to 5.4 times more debris compared to unburned areas, as reported by Santi and Morandi (2013).

The Alps, due to the long history of intense urbanization and to their central position, are a particularly well-studied mountain range with respect to debris-flow hazard, with a rich literature on the related phenomena (e.g., Mueller and Loew 2009, Tiranti et al. 2016). The low-altitude regions are characterized by a temperate climate, with high-intensity short-duration rainfall events which cluster in the Spring and Summer seasons. Debris-flow records follow the same pattern (e.g., Hürlimann et al. 2003, Marchi et al. 2002).

Typically, post-fire debris flows are associated with Mediterranean climates, such as those encountered in the southern European countries, or in the southwestern United States (Esposito et al. 2023). The State of California is particularly prone to wildfires, and early-warning systems take into account the change in susceptibility in burned areas (Staley et al. 2013). In the Alps, large fires are relatively rare, and warning systems do not usually consider wildfire occurrence (Tiranti et al. 2019). However, the frequency and distribution of wildfires appear to be varying due to climate change (Venäläinen et al. 2014). In this context, collecting high-quality data about post-fire debris flows is crucial to maintain a dataset against which hazard-assessment models can be validated.

In this study, we present data and analysis related to the mud-debris flow (according to the classification of Hungr et al., 2014) that occurred on June 7th 2018 in Bussoleno, Northwestern Italy. The municipality is located in the Piedmont region (see Fig. 1), in the central part of the Susa valley. This valley is one of the main connections between Italy and France, thus playing a central role in the European transportation network.

The mud-debris-flow event was triggered by very unusual conditions for the region. In Autumn 2017, large wildfires ravaged the Northern side of the Susa valley, fuelled by a particularly long drought, and by warm foehn winds. This was followed by a very wet Spring season in 2018. Eventually, a thunderstorm triggered the event of June 7th. The basin where the flow originated had shown no sign of activity for at least the precedent 50 years, according to the local information and news sources, and the alluvial fan had been

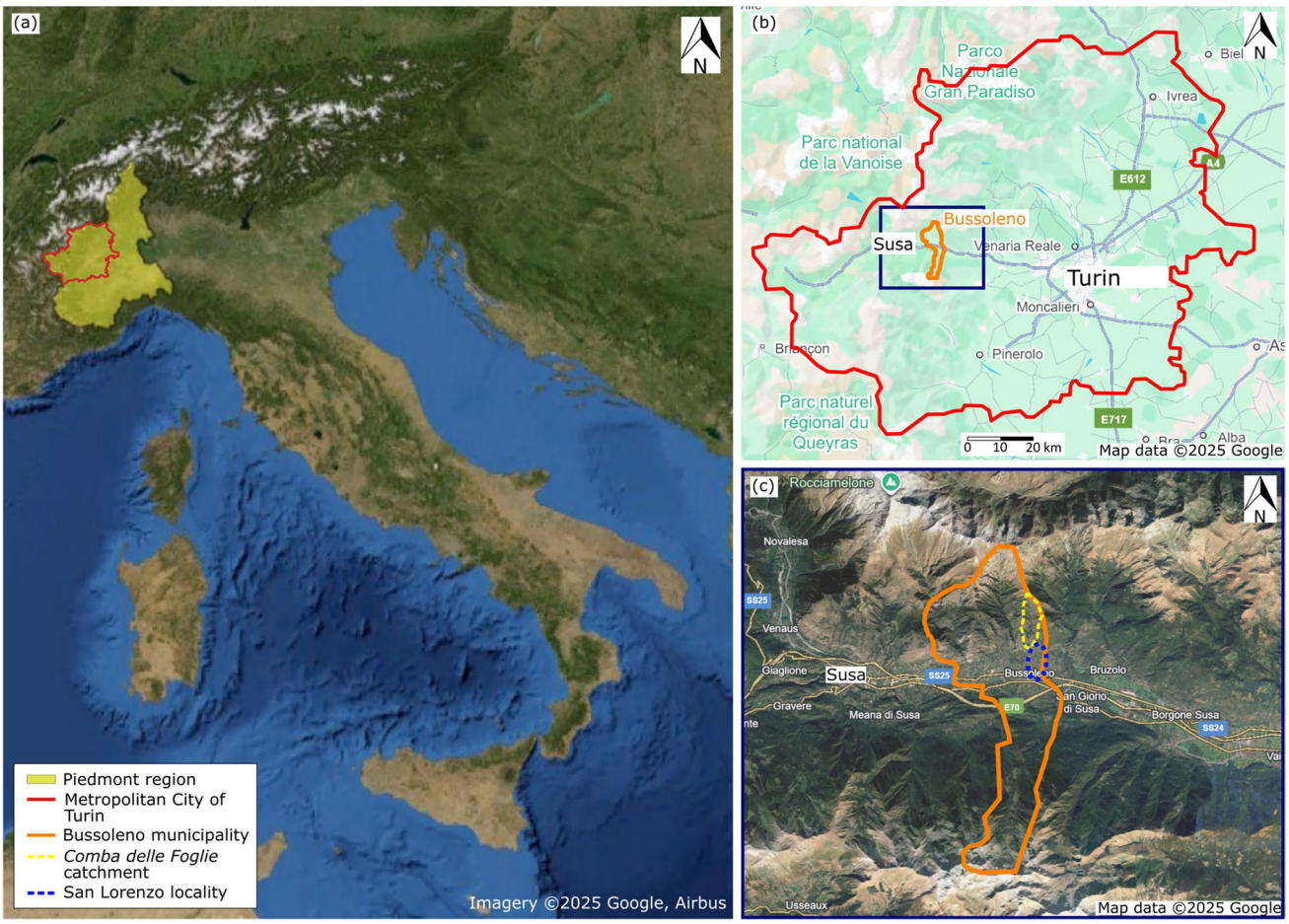

Fig. 1 Geographic context of the study area. **a** The Piedmont region in Italy; **b** the Metropolitan City of Turin, showcasing the town of Bussoleno; **c** a detailed view of Bussoleno, emphasizing the *Comba delle Foglie* catchment and the San Lorenzo locality, interested by the debris flow of June 2018

fully urbanized. Thus, the material mobilized by the combination of wildfire and precipitation had no natural discharge channel and flooded the settlement. The event damaged the municipality of Bussoleno, causing no fatality, but flooding a dozen houses and causing the evacuation of around 150 people (Regione Piemonte 2018). After the event, significant mitigation measures were implemented to prevent damage from future events.

In this work, the numerical back-analysis of the debris-flow event is carried out using two distinct approaches. The first, referred to as *Simplified triggering*, adopts a commonly used method for simulating real events. This involves modeling the runout of a concentrated triggering mass, using a depth-averaged numerical model that treats the flow as an equivalent single-phase material. The aim is to determine the most appropriate rheology to replicate the observed behavior of the event.

However, field evidence indicates that post-fire debris-flow initiation is not confined to a single location but rather involves widespread erosion processes and sediment entrainment throughout the affected catchments (e.g., Rengers et al. 2021, Kean et al. 2013). This aspect was confirmed for the case study (Vacha et al. 2021). To address this, the second approach, referred to as *Susceptibility-based triggering*, incorporates a preliminary susceptibility analysis that accounts for the effects of wildfire on soil properties, including extended fire severity. The same numerical model is then used to simulate the runout under these more realistic conditions, and the results are compared to those of the simplified approach to assess their relative accuracy.

Finally, the best-fit runout simulation after the simplified triggering approach is repeated with the inclusion of the mitigation structures installed after the event. This step is undertaken to evaluate the effectiveness of these measures in mitigating potential future debris flows and to provide insights into the settlement's resilience under similar hazard scenarios.

The article begins with an overview of the topographical and geological characteristics of the *Comba delle Foglie* basin. This is followed by an analysis of the predisposing factors, including the Autumn 2017 wildfire and the rainfall event leading up to the debris flow. The subsequent section details the aftermath of the event, focusing on the extent of the flooded area and the associated socio-economic impacts. The study concludes with the numerical simulations, providing insights into the flow's material properties and its impact on the affected structures.

The Comba delle Foglie catchment

The *Comba delle Foglie* is a small fan-shaped catchment, part of the Susa valley, and drained by the Dora Riparia, one of the early tributaries of the Po river (Fig. 1). It is entirely located in the municipality of Bussoleno, itself a constituent of the Metropolitan City of Turin. The Dora Riparia river crosses the municipality on its south border. A portion of the municipality of Bussoleno, and specifically the locality of San Lorenzo, is located on the alluvial fan of *Comba delle Foglie*.

The watershed extends over 1.37 km^2, at an altitude between 490 and 1790 m a.s.l. (Vacha et al. 2021). The uppermost slope is located just below the *Truc del Vento* peak. The basin is characterized by steep slopes (average slope of 32°, see Fig. 2). The centreline of the basin is characterized by sharp changes in slope inclination, especially between 800 m a.s.l. and the fan apex.

The Comba delle Foglie watershed is geologically complex, as it lies at the structural boundary between two major Alpine tectonic units: the Upper Unit of the Dora-Maira Massif (DM) and the Lower Piedmont Zone (SU) (Vacha 2021). The lower part of the basin primarily overlays the Dora-Maira unit, and in particular its carbonate metasedimentary bedrock, composed of dolomitic marbles and subordinate carbonate-rich calcschists, which are prone to weathering into clay-rich and fine-grained detrital material. Additional lithologies in this sector include micaschists and gneiss from the pre-Triassic basement (DMb), along with Mesozoic calcschists and marbles from the DM cover sequence (DMc). In contrast, the upper sectors of the catchment are dominated by lithologies derived from the SU, such as serpentinites, serpentinoschists, chloritoschists, and additional calcschists. These geological formations reflect a complex tectonic history and contribute to the variability of weathering processes, soil formation, and sediment availability within the catchment.

To characterize the surficial material, a total of 11 soil samples were collected across the catchment and analyzed for particle-size distribution (Vacha 2021). The soils are predominantly sandy in texture, with a variable fraction of gravel and fines. Based on the Unified Soil Classification System (USCS), most samples fall into the SM group (silty sand), with fines content ranging from 5 to 7%. Other samples, exhibiting fines below 5%, were classified as GP (poorly graded gravel), GW (well graded gravel), or SP (poorly graded sand), depending on the dominant coarse fraction.

Before the wildfire, the upper part of the basin was covered by sparse vegetation, with a few scattered trees. The bedrock outcropped discontinuously, and the soil layer was very shallow, reaching only a few centimeters in depth (Vacha et al. 2021). According to the Clay Weathering Index (CWI) adopted in Piedmont Region after Tiranti et al. (2014), the predominance of carbonate-rich lithologies qualifies the basin as Good Clay Maker (GCM). This designation reflects the high propensity of these formations to produce clay-rich weathering products, which are particularly susceptible to mobilization. When mobilized, these fine-grained sediments typically generate cohesive, viscoplastic debris flows characterized by high fine content and a limited coarse fraction.

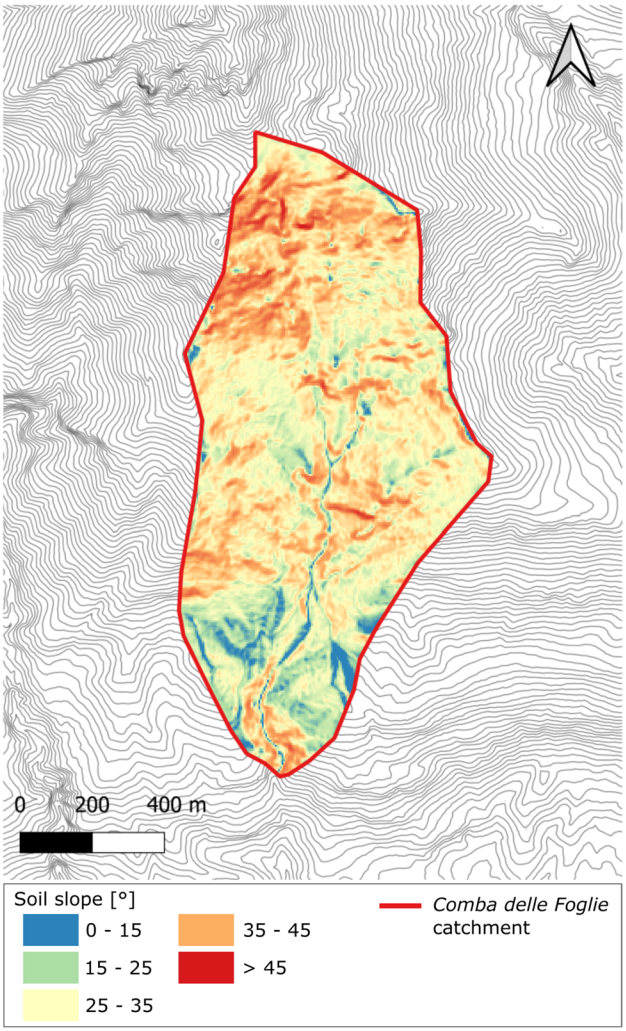

Fig. 2 Slope angle distribution in the *Comba delle Foglie* basin

Wildfire records

In October 2017, the Piedmont region experienced exceptional weather conditions. According to a technical report by local authorities (Arpa Piemonte 2017), air temperatures exceeded the 1971–2000 average by approximately 3 °C. Additionally, it was the driest period in the last 60 years. As a result, most days of the month had wildfire alerts. At the end of October, intense and extensive wildfires ravaged the northern Susa Valley. The total area hit by the wildfire was about 40 km^2. In the municipality of Bussoleno, the wildfire was active from October 22nd to November 1st (Vacha et al. 2022). The wildfire mitigation efforts were hampered by strong foehn winds, with maximum wind gusts reaching 90 km/h on multiple consecutive days (Arpa Piemonte 2017).

The regional government conducted post-wildfire site surveys to assess fire severity, producing a fire severity map following the US FIREMON framework (Key and Benson 2006; Regione Piemonte 2019). The initial assessment, carried out immediately after the fire, evaluated tree mortality and fuel consumption, classifying the *Comba delle Foglie* basin as severely affected in its upper portion and moderately affected in the lower part. Overall, more than 95% of the catchment area was burned. A subsequent assessment of fire severity, conducted during the first growing season after the wildfire by Morresi et al. (2022), indicated a good ecosystem response and a significant recovery across the affected

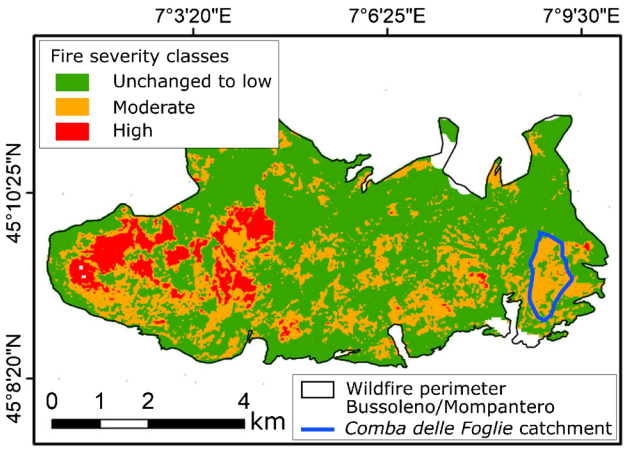

Fig. 3 Fire severity map based on the extended post-wildfire analysis of the affected area (modified from Morresi et al., 2022)

area. Figure 3 presents the extended fire severity map, which was used to analyze soil conditions at the time of the 2018 debris-flow event.

The 2017 wildfire caused the increase of available loose material prone to instability and modified the hydro-mechanical characteristics of the slope. The fire, characterized by significant spatial variability in burn severity, affected large portions of the *Comba delle Foglie* catchment, including areas that had been impacted by earlier fire occurrence. This overlapping disturbance regime resulted in widespread degradation of vegetation and soil cover, particularly in the upper and middle sectors. Post-fire field surveys documented extensive erosion features, including both areal surface erosion and incision along zero-order streams and the main drainage axis (Vacha 2021). In the central channel, morphological evidence of sediment transport — such as scour zones, lateral levees, and debris deposits — was observed from the initiation area to the basin outlet.

To quantify the mechanical effects of wildfire, in situ shear strength tests were conducted on burned and adjacent unburned soils (Vacha 2021). Results showed a pronounced decrease in shear resistance in burned soil areas, with values reduced by approximately a factor of three. This reflects the loss of apparent cohesion due to root system combustion and confirms the mechanical weakening of surface soils. Hydrologically, Water Drop Penetration Time (WDPT) testing in high-severity burn zones indicated localized water repellency within the upper soil layers, potentially limiting infiltration during rainfall events. Measurements of soil thermal conductivity further revealed that heat penetration was largely restricted to the upper 10 *cm* of soil, the most critical zone for both hydrological response and slope reinforcement. The combination of these post-fire effects — mechanical weakening, infiltration reduction, and increased sediment availability — significantly enhanced the catchment susceptibility to debris-flow initiation under moderate rainfall conditions.

Rainfall records and debris-flow triggering

The study area lies within the transition from the humid subtropical climate zone of the Northern Italian plain to the cold continental climate region of the Alps. These are both characterized by the absence of a dry season and by warm summers.

The year preceding the event of June 7th 2018 was marked by two distinct climate anomalies. With respect to the reference period 1971–2000, the year 2018 was particularly warm, with a thermal anomaly of 1.6°C. However, a temperature oscillation was observed during the months preceding the event: from the end of February to March, a negative trend with respect to average values of the reference period was measured, followed by an April characterized by the warmest deviation, of around 3.5°C. On the other side, the low-rainfall anomaly of Autumn 2017 was followed by an exceptionally rainy year in 2018 (Fig. 4). The average cumulative rainfall was about 1380 mm, exceeding of 332 mm the norm of the reference period 1971–2000. The spring of 2018 registered an average rainfall of 463 mm, 40% larger than in the reference observation frame 1971–2000. Additionally, May 2018 registered a 60% rainfall surplus with respect to the period 1971–2000. In particular, in the middle Susa Valley (where Bussoleno is located), 30 days with rainfall were recorded in the period between April 29th and June 7th (Vacha et al. 2021).

The two months preceding the event exhibited a reactivation of the runoff release from the basin. On April 29th 2018, Bussoleno was flooded by mud and water coming from *Comba delle Foglie*, reaching the alluvial fan. The lack of any functional drainage system was made evident at that time: the medieval drainage channel had been removed due to poorly-regulated urbanization in the 60s. Thus, mud and debris preferentially followed paths given by the steepest paved roads, which were damaged. Then, on May 2nd, 9th and 13th, debris flows and floods were recorded, but limited quantities of debris and charred driftwood reportedly reached the settlement. Instead, according to Vacha et al. (2021), a survey conducted on June 5th (two days before the main event) showed accumulated debris on the channel, and particularly at the bottom of the last cliff above the fan apex, which may have been caused by the minor debris-flow events cited.

Prolonged and persistent rainfall in the weeks preceding the June 7 event likely played a key preparatory role in destabilizing the basin. Cumulative precipitation led to progressive saturation of the soil profile, which had already been compromised by wildfire-induced hydrophobicity and structural degradation. These antecedent conditions reduced the infiltration capacity and promoted surface runoff, thereby weakening slope stability. As a result, the

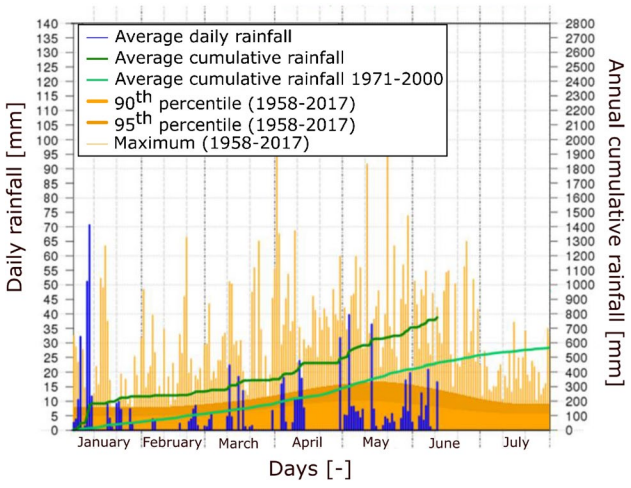

Fig. 4 Daily rainfall trends in the Susa Valley in 2018 compared to the 1971–2000 climatic norm (modified from Arpa Piemonte, 2018)

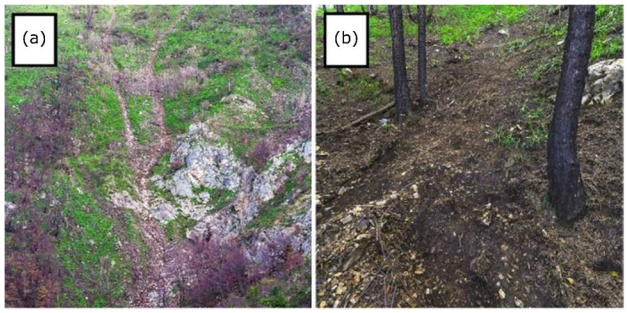

Fig. 5 Photographs illustrating erosion processes observed in **a** the low-order drainage and **b** the open slope (modified from Vacha et al., 2021)

catchment became increasingly susceptible to debris-flow initiation, even under moderate-intensity storms. Furthermore, the minor flows and floods of the months preceding the main event of June may have contributed to its severity by mobilizing debris towards the main channel of the basin, which were then reactivated.

Debris-flow dynamics and field surveys

The wildfire induced significant alterations in the *Comba delle Foglie* basin, resulting in a heterogeneous distribution of fire effects. In certain areas, bare soil was exposed before the debris-flow event, while in others, new vegetation had begun to regrow on the charred ground. Scattered zones of erosion-prone and highly susceptible soil were identified within the catchment.

Likely, on June 7th, the debris flow triggered at the upper part of the basin, where post-event observations revealed rill formation converging toward the centerline (Vacha et al. 2021). The lower section of the basin displayed evidence of erosive processes and sediment transport (Fig. 5a), while sheetflow erosion was observed on open slopes (Fig. 5b).

Regarding the rainfall that triggered the landslide, the closest rain gauge to the study area, the Prarotto station, recorded low intensities around the time the debris flow was initiated and propagated. However, this station is located 7 km from the *Comba delle Foglie*. On the other hand, radar weather provided additional measurements. According to data estimated by the *Bric della Croce* radar, between 11:55 and 12:25 UTC (around the debris flow occurrence time) an average cumulative triggering rainfall of 12 mm in 30 min was measured (24 mm/h), corresponding to a return period of 5 years (Tiranti et al. 2014), as shown in Fig. 6. Although a GCM basin like *Comba delle Foglie* typically experiences the triggering of shallow instabilities with rainfall intensities higher than 30 mm/h (Tiranti et al. 2014), wildfires have reasonably reduced the triggering rainfall threshold (Tiranti et al. 2021). However, it is worth pointing out that the reliability of these radar data is affected by limited visibility due to the complex orography of the area.

In Fig. 7, the nature of deposits of the mud-debris flow is appreciable. The flow deposition interested an area of around 35,000 m^2 in the alluvial fan (Figs. 8 and 9), and showed a deposited maximum flow height of 2 m. A double flow behavior of the coarser and finer material was observed during the event (Fig. 8). The coarser material, characterized by higher energy during the runout, deposited with a material height of 1 to 1.5 m at obstacles (e.g., buildings), and 30 to 60 cm otherwise. On the other side, the flow of the finer material showed a longer runout in the inhabited area, with a deposited average flow height of 5 to 10 cm, and between 50 and 60 cm at obstacles (Arpa Piemonte 2018). It advanced as far as the valley's main railway line. The maximum flow height at the buildings was measured post-event at selected survey points. The measurements

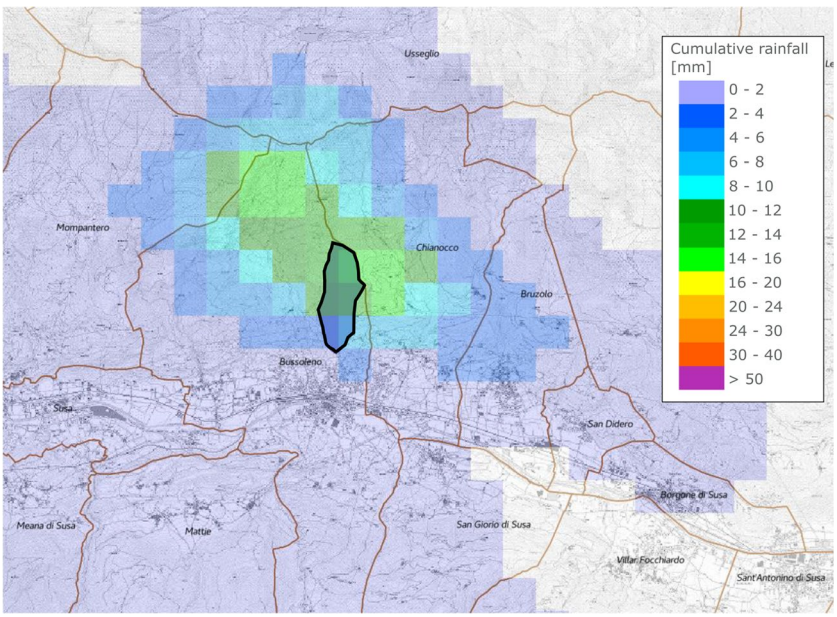

Fig. 6 Cumulative rainfall [mm] estimated from observations of the Bric della Croce radar, for the time interval 11:55–12:25 UTC on 7th June 2018 (modified from Regione Piemonte, 2018). The *Comba delle Foglie* basin is highlighted in the picture

Fig. 7 Deposits from the June 2018 mud-debris-flow event (bottom photograph modified from Vacha, 2021)

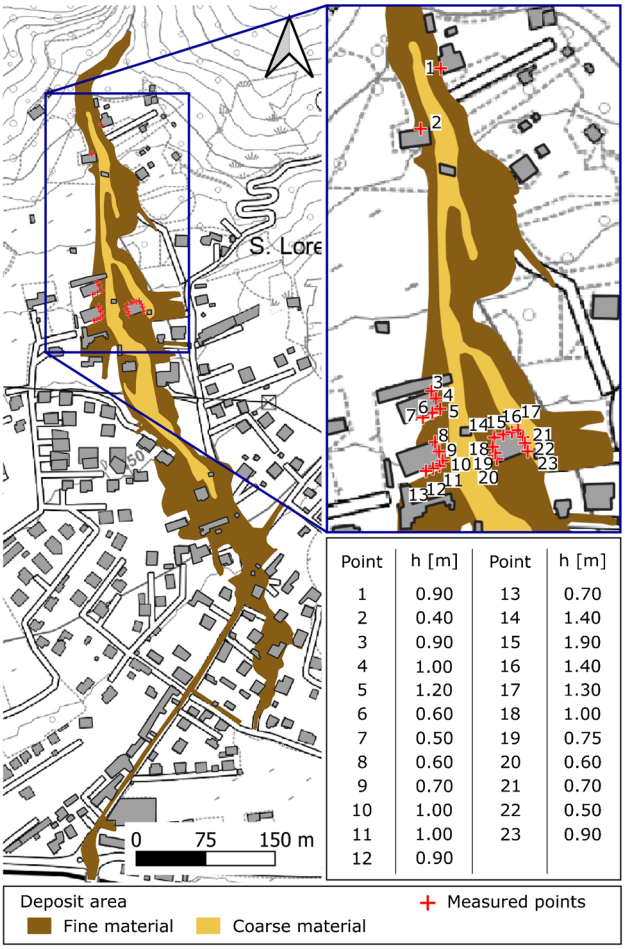

Point	h [m]	Point	h [m]
1	0.90	13	0.70
2	0.40	14	1.40
3	0.90	15	1.90
4	1.00	16	1.40
5	1.20	17	1.30
6	0.60	18	1.00
7	0.50	19	0.75
8	0.60	20	0.60
9	0.70	21	0.70
10	1.00	22	0.50
11	1.00	23	0.90
12	0.90		

Fig. 8 Surveyed flooded area (modified from Arpa Piemonte, 2018) and flow heights during the event of June 2018

and their corresponding locations are presented in Fig. 8. Overall, the estimated deposited material at the alluvial fan was 15,000 to 20,000 m^3.

The debris flow caused numerous socio-economic impacts, although no casualties were reported. The event resulted in the destruction of two buildings and caused severe structural damage to two others. Additionally, more than ten buildings experienced functional impairments. Critical infrastructure, including the supply of electricity, potable water, and domestic gas, was disrupted, and approximately 150 residents were evacuated. Since the debris-flow event of June 7, 2018, no further signs of reactivation or new debris flow occurrences have been reported in the *Comba delle Foglie* catchment. This observation is based on both field surveys and the absence of documented reports from Regional Authorities or Local Stakeholders.

Mitigation measures post event

Following the debris-flow event of 2018, a series of structural mitigation measurements were implemented to channel the flow toward the main valley river, the Dora Riparia, ensuring controlled discharge and reducing the impact on urbanized areas.

Active measures focused on improving the stability and resilience of the terrain. These interventions primarily involved the restoration of vegetation cover, serving multiple critical functions. Vegetation enhances the mechanical properties of the soil by increasing its shear strength through root reinforcement, reduces surface erosion, and captures meteoric water. The reforestation and revegetation strategies were carefully selected to match the local ecological and climatic conditions to ensure long-term effectiveness.

Passive mitigation measures were also integral to the overall risk reduction strategy. These measures were designed to dissipate the energy generated by potential debris-flow events and to contain the resulting materials, thereby protecting critical infrastructure and settlements located downstream. The passive interventions were placed along the flow path, from the source basin to the alluvial fan, and included a series of engineered structures with complementary functions.

The key passive measures implemented at the valley bottom are listed below (Fig. 10):

- One single filter barrier was strategically installed to intercept and retain coarse debris, thereby reducing the volume of solid material transported downstream (Fig.10a and b). The structure is 15 m in width and composed of vertical steel tubes, each 2 m high and spaced 1 m apart. It is anchored to the subsurface using 3-m-long micropiles — in situ cast, reinforced concrete piles — which provide enhanced foundational stability and load-bearing capacity.

Fig. 9 Photographs documenting the debris-flow event of June 2018: the images show the flooded area and the affected buildings. The red arrow indicates the flow direction, while the blue circles mark the locations of destroyed structures

- Two check dams were constructed to contain high-energy debris flows and to withstand significant dynamic impact forces associated with such events (Fig. 10a and c). These dams are made of compacted soil and lined with large boulders. The upstream dam is 50 m wide and 6 m high, with an estimated sediment storage capacity of approximately 7000 m^3. Embedded drainage pipes facilitate controlled water discharge. The downstream dam is 100 m wide and 2.5 m high, offering a storage capacity of about 6000 m^3. It is similarly equipped with internal drainage pipes to manage water flow and maintain structural integrity.
- Three sediment and water retention basins have been constructed to attenuate peak discharge and mitigate downstream flooding (Fig. 10a). The total combined storage capacity of these basins is approximately 10,000 m^3, effectively reducing peak discharge from 10 m^3/s to near zero during high-intensity events.
- The existing river channel was reconfigured to enhance its hydraulic capacity and flow conveyance, thereby minimizing the risk of overflow and sediment deposition in vulnerable zones (blue line in Fig. 10a). The redesigned channel has an average depth of 1.5 m and a width of approximately 3 m, extending over a total length exceeding 2 km. It includes both open-air and culverted sections and is equipped with newly installed infrastructure, including bridges, protective fencing, and stone revetments, to ensure long-term performance and stability.

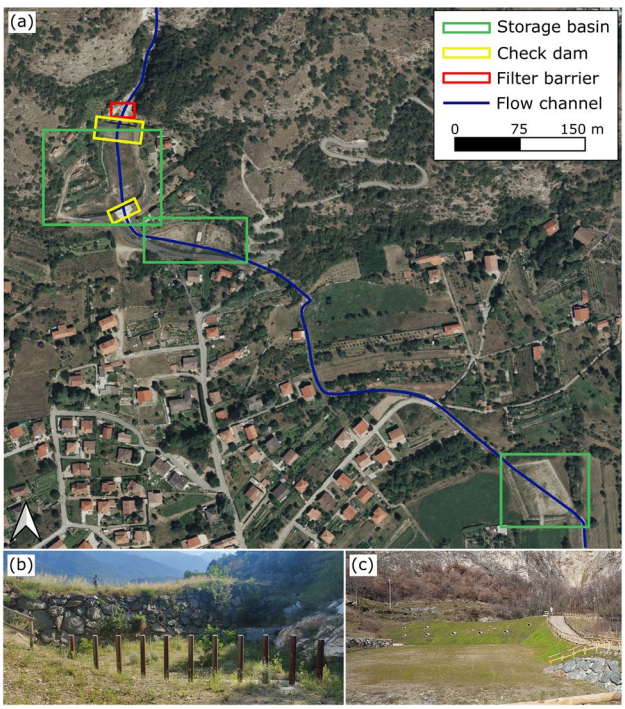

Fig. 10 **a** Location of selected mitigation structures implemented in Bussoleno following the June 2018 debris-flow event, with the new flow channel highlighted in blue; **b** filter barrier; **c** close-up view of a check dam featuring drainage holes

Runout numerical simulations

The back-analysis of the Bussoleno debris flow was conducted by simulating the runout of two distinct triggering scenarios, detailed in the following sections. Before, the numerical model used for the runout simulation, RASH3D, is introduced.

RASH3D, developed by Pirulli (2010), is a numerical model based on a single-phase integrated solution of the St. Venant equations using the shallow water flow assumption. Equations are solved with an Eulerian Finite-Volume scheme. For a more detailed description of the model, readers are referred to Pirulli and Mangeney (2008) and Pirulli and Pastor (2012), along with the references therein.

A runout simulation requires as input the Digital Elevation Model (DEM) of the site, the initial location and volume of the mass to release, and the rheological properties of the material. For the study area, a 5 m × 5 m DEM is provided by the Regional Government. In addition, a 1 m × 1 m LiDAR point cloud is available at a lower altitude. Further details regarding the characteristics and availability of the DEMs are provided in Appendix. For the simulation purposes, the two grids are merged and re-sampled to obtain a DEM with spacing 5 m on the catchment, reducing to 2 m on the

fan area, and to 1 m on the settlement. The obtained computational grid is then refined at the critical areas (e.g., fan apex, around buildings, along the flow path), to accurately analyze and simulate the interaction mechanism of the flow with topography and structures (Leonardi et al. 2021).

According to the geological description in "The Comba delle Foglie catchment" section, the solid fraction of the flow should be mostly composed of fine material. Burned driftwood is expected to be the main source of coarse material. This is confirmed by the post-event survey on the deposits on site.

In RASH3D, mud and debris are homogenized into a single-phase equivalent continuum and described as such. The rheological parameters used in the runout simulations implicitly account for the combined influence of interparticle interactions, excess pore pressures, and water content. One of the limitations of this approach is the impossibility to separate coarse and fine material, which is observed in the field. In fact, coarse grains tend typically to deposit early, while fines are transported by water on very gentle slopes. However, literature widely confirms how single-phase models are able to capture the most relevant features of the flow, such as the final deposit, the flooded area, and the flow speed.

Simplified triggering

The first proposed approach for the release of the mud-debris flow consists on the runout simulation of a concentrated triggering mass, which corresponds to the approach commonly adopted in the literature.

Based on on-site surveys, the triggering volume is 20,000 m^3, and the concentrated mass has a constant thickness. It is positioned along the centerline of the basin (Fig. 11a), at the intersection of the secondary hydraulic flowlines. The chosen location is in an area heavily affected by the 2017 fire, and its steep slopes suggest a significant contribution to the supply of debris. The extent of the triggering area is arbitrarily chosen, and the soil thickness is calculated in order to obtain the chosen volume, resulting in an average value of 1.3 m. Then, rheological parameters are back-calibrated from the flow path observed.

Following a long tradition in depth-averaged models, the single-phase approach is coupled with the choice of a simple rheological model for closure. After the *simplified triggering*, two rheological models are considered and compared in the runout analysis to identify the most suitable one for the case study. The first model, the Voellmy law, has been widely used in the back-analysis of numerous debris-flow events (Hürlimann et al. 2017) and is therefore included. The Voellmy rheology expresses the basal shear strength τ_z through combining a Coulomb and a turbulent term accounting for velocity-dependent friction losses. The constitutive equation is reported below:

$$\tau_z = \gamma h \tan\delta + \frac{\gamma v^2}{\xi}. \quad (1)$$

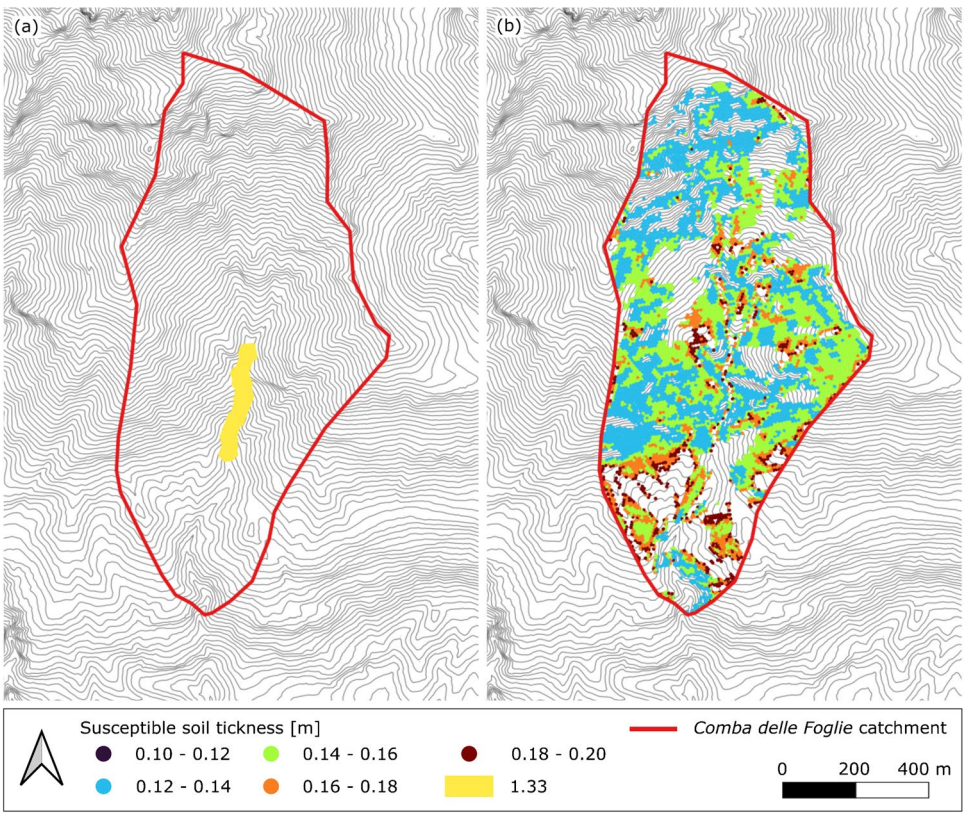

Fig. 11 **a** *Simplified triggering*: triggering volume positioned at the centerline of the basin; **b** *Susceptibility – based triggering*: resulting distribution of the susceptible soil thickness in the *Comba delle Foglie* catchment from the susceptibility analysis

The constitutive parameters are herein the dynamic friction coefficient *tan* δ and the turbolence coefficient ξ (Pirulli et al. 2018). Then, γ is the bulk specific weight, h is the flow depth, and v is the depth-averaged flow velocity.

The second model is the Bingham rheology, which is commonly used to describe the behavior of mud flows (La Porta et al. 2024). This visco-plastic model relates the local shear stress τ_z to the shear rate as:

$$\tau_z = \tau_0 + \mu_B v. \quad (2)$$

The constitutive parameters are the yield stress τ_0, assumed to be equal to the saturated soil cohesion, and μ_B, a post-yield viscosity (Pastor et al. 2004). The second term in Eqs. 1 and 2 incorporates all resistances due to dynamic energy dissipation within the flow.

The rheological parameters can hardly be measured directly, but can be hypothesized from the literature on back-calculations of events that occurred in similar conditions. However, choosing the appropriate couple of parameters is, in this case, particularly challenging. The vast majority of literature cases in the region is not calibrated on a post-wildfire event, as these phenomena

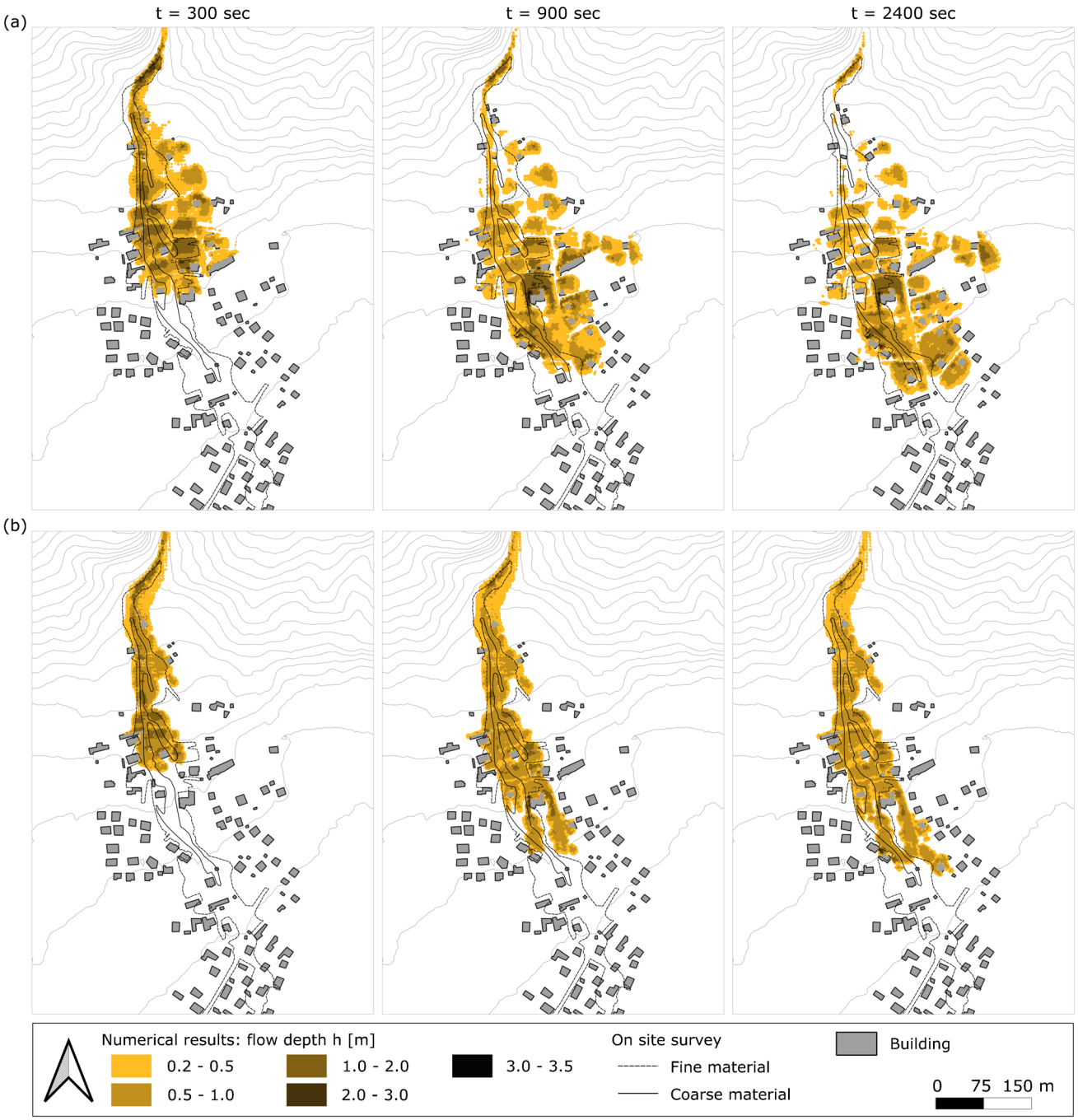

Fig. 12 Simulated runout after the *simplified triggering* approach and comparison with surveyed flooded area: results using **a** a Voellmy rheology with *tan* $\delta = 0.1$and $\xi = 500$ m/s^2, and **b** a Bingham rheology with $\tau_0 = 1300$ Pa and $\mu_B = 80$ Pa·s

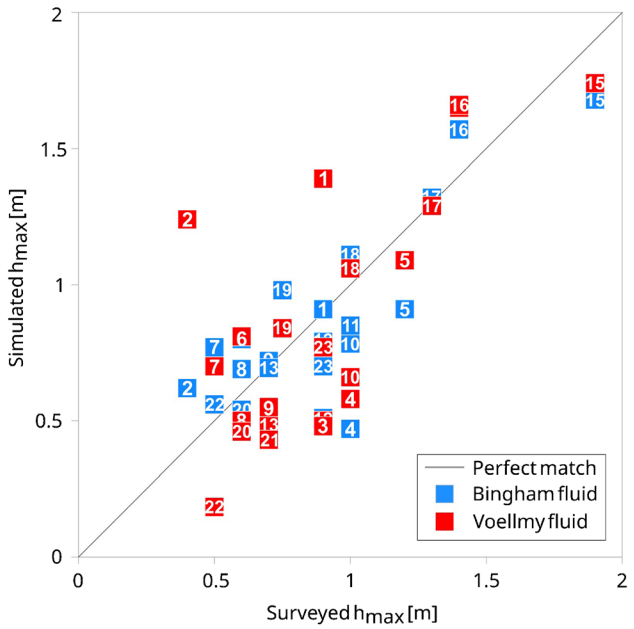

Fig. 13 Quantitative comparison of observed and simulated maximum flow heights. Number of points refers to surveyed flow heights reported in Fig. 8

are relatively rare. Thus, we proceed with an ad hoc calibration. Parameters are calibrated by choosing the values that return a simulated deposit that is in agreement with the survey conducted on site.

All rheological parameters are varied within intervals consistent with the literature (Pirulli et al. 2017; Prochaska et al. 2008; Pastor et al. 2004). For the Voellmy law, $tan\ \delta$ was tested in the range 0.03–0.18, while ξ between 300 and 1500 m/s^2. The best-fit simulation is reported in Fig. 12a, with $tan\ \delta$ being 0.1 and ξ being 500 m/s^2. For the Bingham law, τ_0 was tested between 500 and 1500 Pa, and μ_B between 50 and 600 Pa·s. Figure 12b shows the best-fit simulation considering a Bingham law, with $\tau_0 = 1300$ Pa and $\mu_B = 80$ Pa·s.

The comparison indicates that the Bingham rheology provides the most suitable representation of the observed flow behavior. As shown in Fig. 12, the Voellmy fluid simulation significantly overestimates the flooded area, whereas the Bingham fluid more accurately captures the surveyed flow path of the coarser material, although the path of the finer material is not simulated. Reproducing the pathways of the finer material requires a reduction in rheological parameters, particularly the yield stress (τ_0). However, this adjustment comes at the expense of accurately representing the simulated flow heights. In terms of simulated maximum flow heights, Fig. 13 presents a comparison between the maximum flow heights measured at the survey points shown in Fig. 8 and the simulated results obtained using both rheological models. The graph shows that both rheologies approximate the surveyed values reasonably well, with the Bingham

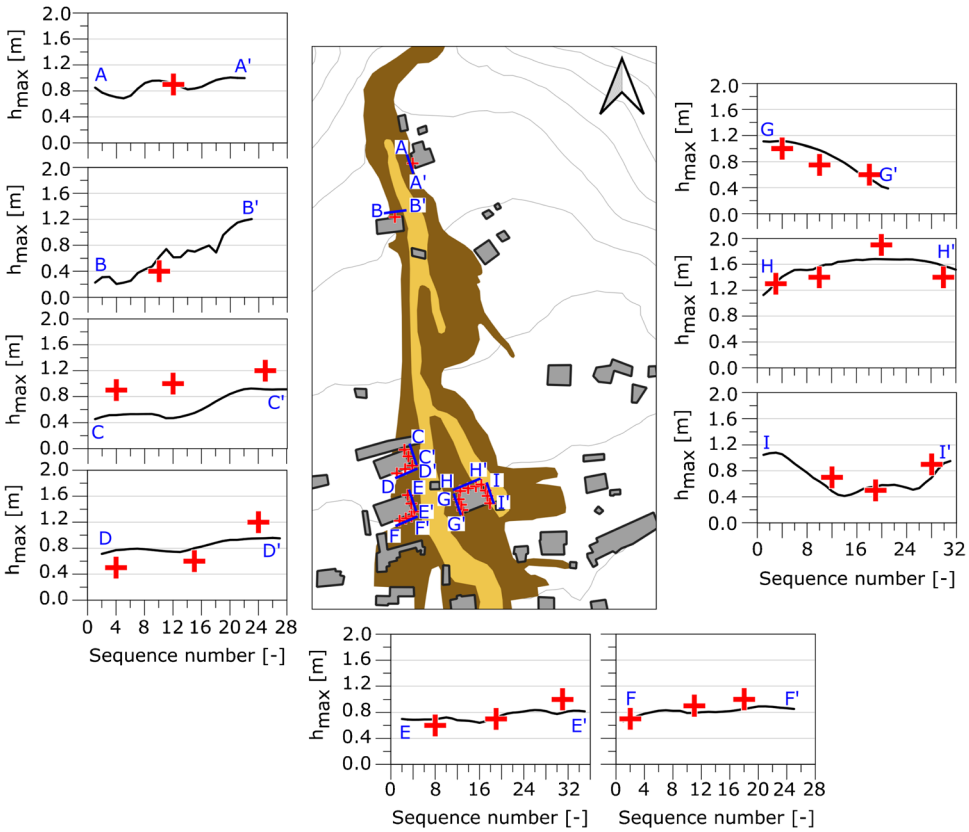

Fig. 14 Bingham simulation with $\tau_0 = 1300$ Pa and $\mu_B = 80$ Pa·s: flow trend at some sections, and comparison with the measured survey points of Fig. 8, indicated by the red plus sign

fluid providing a slightly closer match to the observed behavior. In conclusion, the Bingham rheology is identified as the most appropriate model for replicating the Bussoleno event of 2018.

To better illustrate the Bingham flow behavior in the building area, Fig. 14 presents the simulated flow height profiles along selected sections. These profiles correspond to the survey points shown in Fig. 8, where the simulated flow trends closely match the measured data. Thus, the simulations capture the general pattern of the observed flow heights effectively. However, a discrepancy is evident at section CC', where the simulated flow heights are systematically lower than the measurements. This difference is attributed to the destruction of a building located immediately upstream during the June 2018 event, which altered the flow dynamics. In contrast, the simulations assume the building remains intact, as it is included in the DEM without considering structural failure. Consequently, the lower simulated flow heights at this location are consistent with the model assumptions.

In terms of maximum flow velocities, the highest values were reached at the apex of the alluvial fan, in correspondence with a marked slope discontinuity where the channel gradient increases abruptly. In this area, simulated peak velocities reached approximately 20 m/s. In contrast, in the urbanized sector, flow velocities were significantly lower, with maximum simulated values of about 5 m/s. The spatial distribution of maximum flow velocities in proximity to the impacted buildings is illustrated in Fig. 15.

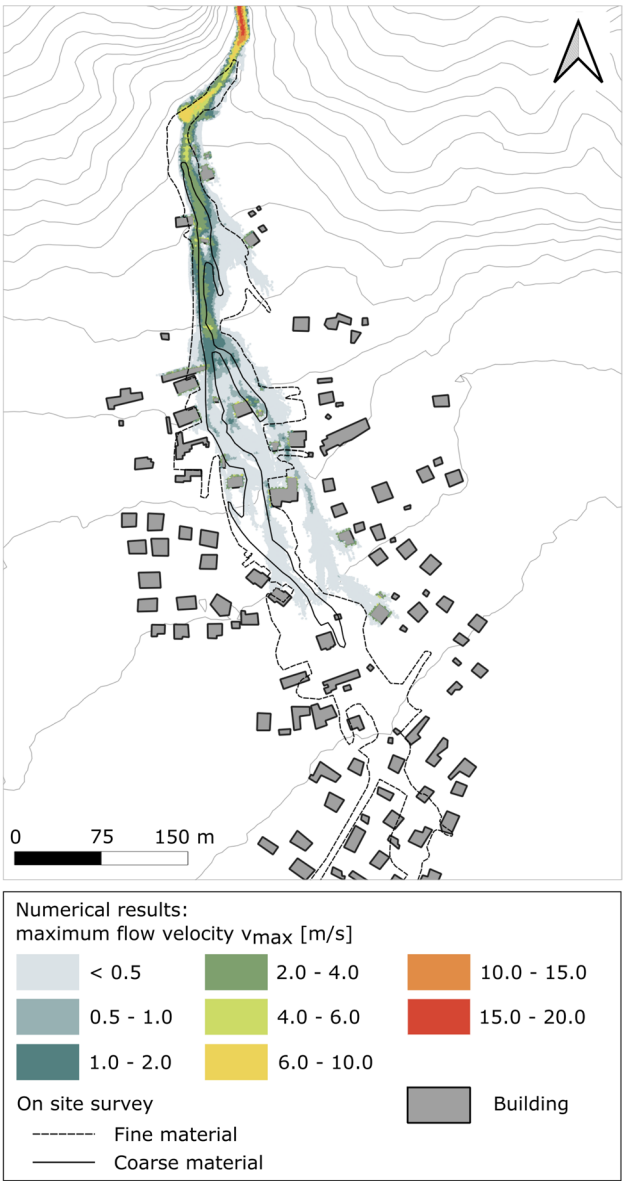

Fig. 15 Simulated flow maximum velocity distribution in the urbanized area, using a Bingham rheology with $\tau_0 = 1300$ Pa and $\mu_B = 80$ Pa·s

Susceptibility-based triggering

As already reported, wildfires significantly alter the hydro-mechanical properties of soils. Consequently, the risk of shallow landslides can increase dramatically (e.g., Gehring et al. 2019). While the simplified approach outlined above effectively captures the flow dynamics once triggered, a susceptibility analysis is crucial for a more detailed assessment of the triggering process.

Numerical modeling of post-fire debris flows must incorporate wildfire-induced soil alterations alongside key driving factors, such as unsaturated soil conditions and root reinforcement. Most existing approaches to assess landslide susceptibility after wildfires rely on empirical, data-driven, or statistical methods, often defining rainfall thresholds above which landslides are likely. However, these thresholds are typically site-specific and fail to account for the physical processes within the soil or the potential effects of climate change on rainfall patterns. While some physics-based post-fire slope stability models have been proposed, they remain complex or omit critical aspects of soil behavior (Abdollahi et al. 2023).

Given the limited data available for the case study analyzed, the authors propose a methodology to carry out the susceptibility analysis under specific assumptions. Many existing models couple mechanical and hydraulic aspects, accounting for pore pressure variations due to rainfall infiltration (e.g., Stancanelli et al. 2017, Thomas et al. 2021). However, the Bussoleno case study is characterized by uncertainty regarding the precise rainfall intensities that triggered the debris flow. Consequently, the authors conducted a purely mechanical susceptibility analysis using the infinite-slope stability model. While pore pressure evolution is not explicitly modeled, the susceptibility analysis assumes fully saturated soil conditions. This assumption reflected the observed antecedent hydro-meteorological conditions, including prolonged rainfall and reduced infiltration capacity due to wildfire-induced soil modifications.

Slopes steeper than 45°, where exposed bedrock is present, are considered unconditionally stable and excluded from the analysis. Furthermore, cells within the *Comba delle Foglie* basin are filtered using the extended fire severity map shown in Fig. 3, to take into account the mapped severity of the wildfires, including the recovery capacity of the catchment. Areas marked as green in the map are excluded from the susceptibility analysis and considered as stable. In the remaining areas, the superficial soil layer is assumed to be susceptible to instability when saturated. This assumption is supported by site surveys conducted in the days preceding the event,

which documented widespread scouring and erosion throughout the basin (Vacha et al. 2021).

Following Stancanelli et al. (2017), the limit equilibrium conditions are evaluated for each DEM point within the basin, based on the local slope angle ψ. A simple Mohr-Coulomb failure criterion is employed to determine the thickness of the unstable soil layer h_0 using the following equation:

$$h_0 = \frac{c}{\gamma \sin\psi \cos\psi - (\gamma - \gamma_w)\cos\psi^2 \tan\phi}, \quad (3)$$

where c and ϕ are the soil cohesion and friction angle, γ and γ_w are the specific weight of the saturated soil and water, respectively.

To reflect the shallow nature of soil alterations caused by wildfires, the maximum thickness of the unstable soil layer is capped at 0.2 m. This constraint is supported by literature findings indicating that wildfires primarily affect only the superficial soil layer due to the limited penetration of thermal gradients during extreme events (Chicco et al. 2023).

Experimental studies have investigated the impact of wildfires on the mechanical properties of soils (Secci et al. 2014; Lei et al. 2022; Peduto et al. 2022). Although these studies involve different soil types, they consistently report that wildfires have a negligible effect on the frictional strength of soils. However, they cause a significant reduction in cohesion (c) due to root decay. Additionally, Lei et al. (2022) observed that the mechanical properties of fire-affected soils deteriorate progressively over time, with pronounced declines noted in samples collected 2 months, 1 year, and 2 years after a wildfire. Therefore, for the current analysis, an average soil friction angle (ϕ) of 22° was assumed. Cohesion (c) was set to the residual value contributed by vegetation roots following a wildfire. Based on literature data (e.g., Abdollahi et al. 2023), a residual cohesion value of 1 kPa was adopted.

The distribution of unstable cells within the *Comba delle Foglie* catchment, calculated using the described methodology, is presented in Fig. 11b. The results indicate that the majority of cells within the basin are classified as unstable, with the thickness of susceptible soil layers ranging between 0.1 and 0.2 m.

The infinite-slope stability analysis estimates a susceptible soil volume of approximately 84,000 m^3. To simulate the runout of this mobilized mass, the rheological parameters calibrated in the previous section are applied: the material is modeled as a Bingham fluid with a yield stress (τ_0) of 1300 Pa and a viscosity (μ_B) of 80 Pa·s. Using this configuration, the simulation indicates that around 16,000 m^3 of material reach the alluvial fan and flow into the urbanized area (Fig. 16).

A comparison between Fig. 12b, which depicts the runout of a concentrated mass of 20,000 m^3, and Fig. 16, which shows the runout of the susceptible areas identified through the susceptibility analysis, highlights similar deposition patterns in the settlement. With respect to the runout of the simplified triggering, the simulated flow in Fig. 16 demonstrates lower intensity: after 300 s, no material has yet reached the village, and in subsequent time steps, the flow propagates with reduced energy. This slower propagation results in a more controlled runout path and a longer

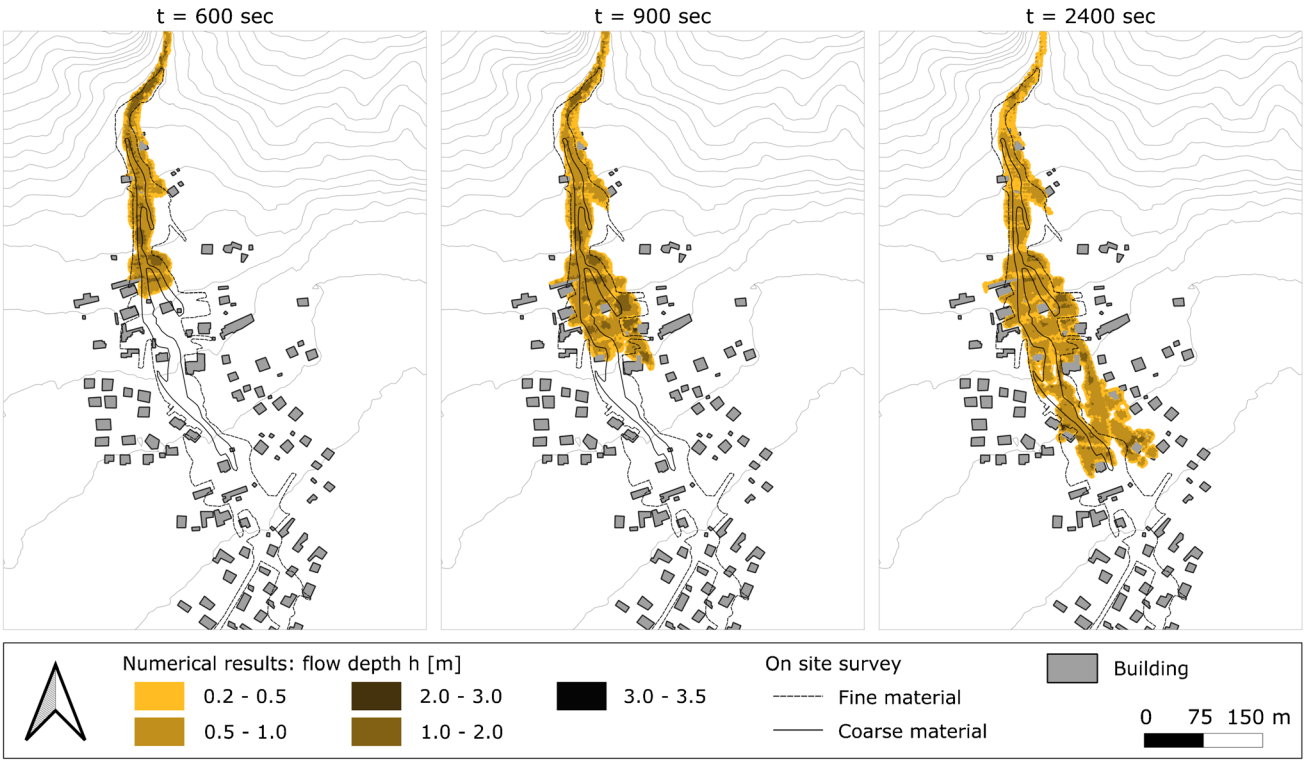

Fig. 16 Simulated runout after the *susceptibility – based triggering* approach, adopting the Bingham rheology with τ_0 = 1300 Pa and μ_B = 80 Pa·s. In this case, the flow does not reach the settlement within the first 300 s. At 600 s, a significant portion of the flow begins to affect the urban area

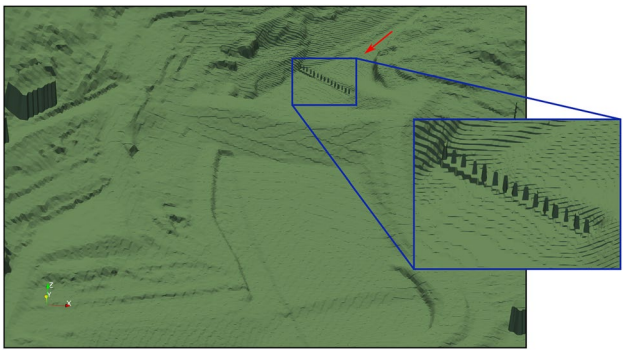

Fig. 17 Filter barrier located at the apex of the alluvial fan: model integration within the DTM used for the simulation. The red arrow indicates the direction of the flow

travel distance along the main channel. The maximum flow heights recorded in both simulations are comparable. The flow resulting from the susceptibility analysis exhibits better alignment with the channelized morphology at the apex of the alluvial fan, providing a slightly more accurate representation of the flow path.

Susceptibility analysis is essential to better understand the effects of contributing and triggering factors on increasing the soil proneness to instability. However, from the comparison, it appears that, for this case study, the flow can be analyzed with good precision using the simplified back-calculation, because the geometry of the case study does not cause evident differences on the two approaches.

Numerical analysis with post-mitigation measurements

A new 1 m × 1 m LiDAR-derived Digital Terrain Model (DTM) was generated after the implementation of mitigation structures, to assess their effectiveness in controlling and containing a debris-flow event similar to that of 2018. The updated DTM incorporates storage basins and check dams and has been further refined to include the filter barrier positioned at the apex of the alluvial fan (Fig. 17). Additionally, the computational grid was locally refined around the edges of the mitigation structures.

To evaluate the behavior of the flow in the presence of the mitigation strategies, the runout of the Bingham fluid following the simplified triggering approach is simulated using the new DTM (Fig. 18). The simulation is performed adopting the same rheological parameters calibrated in the previous back-analysis. It is evident that the involved mitigation structures properly contain the simulated flow volume. The volume of 20,000 m^3 reaches the first two storage basins, accumulating at the perimeter rigid barriers. Since the simulated flow is modeled as an equivalent single-phase fluid, the integrated filter barrier acts in slightly reducing the flow velocity, but it does not significantly affect the deposition pattern.

Conclusions

The debris flow that impacted Bussoleno, a small village in the Metropolitan City of Turin, on June 7, 2018, was an unexpected event that caused significant damage to the existing urbanized area. In response, an extensive mitigation network was implemented, including the construction of multiple mitigation structures aimed at reducing future risks.

Among the predisposing factors of the instability, the October 2017 wildfires in the Susa Valley played a critical role. Wildfires are known to significantly alter the hydro-mechanical properties of soils, thereby increasing their susceptibility to failure under hydrological stress.

This study provides a comprehensive analysis of the event, including the weather conditions that contributed to the triggering of the debris flow and the post-event mitigation strategies that were adopted. Then, the back-analysis of the debris flow is based on two complementary approaches. The first, referred to as *simplified triggering*, simulated the runout of a concentrated triggering mass,

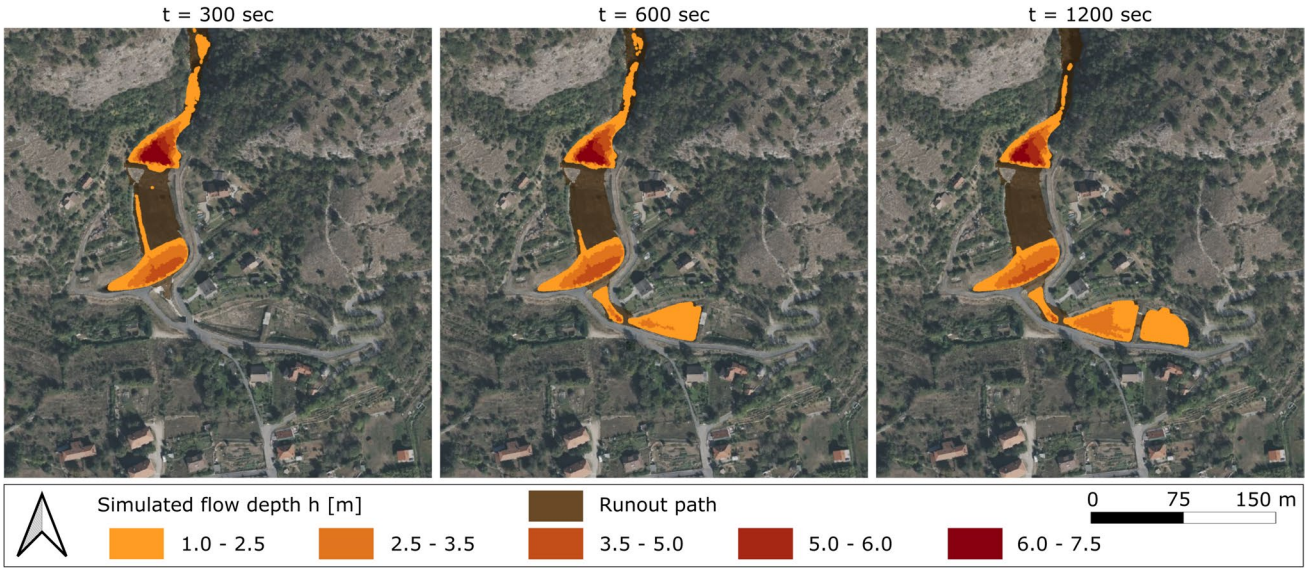

Fig. 18 Simulated runout of the Bingham flow (τ_0 = 1300 Pa, μ_B = 80 Pa·s), after integration of the mitigation strategies

according to the common method used in the literature. The continuum numerical code RASH3D, based on depth-averaged mass and momentum conservation equations, was used. Two rheological models were tested to capture the flow behavior by comparing simulated maximum flow depths and paths with field survey data. Among the tested models, the Bingham rheology proved most suitable, as it effectively reproduced the flow heights and the flow path of the coarser material fraction. However, the single-phase fluid assumption inherent in the model limits its ability to simulate the finer material's behavior accurately.

The second approach, referred to as *susceptibility-based triggering*, incorporated field observations that indicated distributed triggering across the catchment. A simplified susceptibility mapping method was proposed. This approach is constrained by the limited availability of data on the soil's hydro-mechanical state and rainfall conditions before and during the event. A mechanical analysis based on the infinite-slope stability model was performed, incorporating assumptions derived from literature to address the data gaps. Then, runout simulations with RASH3D were conducted using the previously calibrated rheological properties on the Bingham fluid. From the comparison of the two methods applied on the runout, the simulated maximum flow heights resulted to be comparable. However, the simulation using the susceptibility-based triggering more accurately depicted the flow path. Although the susceptibility analysis offered a valuable instrument to enhance the precision of the back-analysis, the simplified methodology demonstrated good reliability for the studied event.

Finally, the effectiveness of the implemented mitigation network was evaluated through a runout simulation after the simplified triggering approach, performed on a post-event Digital Elevation Model (DEM) that included the constructed mitigation structures. The back-calibrated Bingham fluid model demonstrated that the flow was contained by the mitigation measures closest to the fan apex, underscoring the efficacy of these structures in managing future events of similar magnitude to the design scenario of the 2018 debris flow.

Acknowledgements

This study was partially carried out within the RETURN Extended Partnership and received funding from the European Union Next-GenerationEU (National Recovery and Resilience Plan – NRRP, Mission 4, Component 2, Investment 1.3 – D.D. 1243 2/8/2022, PE0000005) – SPOKE VS 2. The authors wish to thank Dr. Mauro Tararbra (ARPA Piemonte) for his support.

Funding Open access funding provided by Politecnico di Torino within the CRUI-CARE Agreement.

Declarations

Conflict of interest The authors declare no competing interests.

Appendix. Description of the DEM datasets

The 5 m × 5 m DEM of the study area was obtained from the *GeoPiemonte* portal (www.geoportale.igr.piemonte.it), the official geospatial data platform of the Piedmont Region. This dataset was generated from an airborne photogrammetric and LiDAR survey conducted using the Leica ALS system. The 1 m × 1 m high-resolution DEM was derived from a LiDAR survey performed using an unmanned aerial vehicle (UAV). This dataset is proprietary and was produced by the authors.

References

Abdollahi M, Vahedifard F, Tracy FT (2023) Post-wildfire stability of unsaturated hillslopes against rainfall-triggered landslides. Earth's Future 11(3), https://doi.org/10.1029/2022EF003213

Arpa Piemonte (2017) Rapporto tecnico sulla qualità dell'aria e sulle attività dell'agenzia a supporto dell'emergenza per gli incendi boschivi in Piemonte nel mese di ottobre 2017. Tech Rep

Arpa Piemonte (2018) Rapporto evento del 07/06/2018. Tech. rep, Colata detritica nel comune di Bussoleno

Chicco JM, Mandrone G, Vacha D (2023) Effects of wildfire on soils: field studies and modelling on induced underground temperature variations. Frontier Earth Sci 11(December):1–12. https://doi.org/10.3389/feart.2023.1307569

Debano LF (2000) The role of fire and soil heating on water repellency in wildland environments: a review. J Hydro 231–232:195–206. https://doi.org/10.1016/S0022-1694(00)00194-3

Doerr SH, Blake WH, Shakesby RA, Stagnitti F, Vuurens SH, Humphreys GS, Wallbrink P (2004) Heating effects on water repellency in Australian eucalypt forest soils and their value in estimating wildfire soil temperatures. Int J Wildland Fire 13(2):157–163

Ebel BA, Moody JA (2020) Parameter estimation for multiple post-wildfire hydrologic models. Hydro Process 34(21):4049–4066

Esposito G, Gariano SL, Masi R, Alfano S, Giannatiempo G (2023) Rainfall conditions leading to runoff-initiated post-fire debris flows in Campania, Southern Italy. Geomorphology 423(December 2022):108557, https://doi.org/10.1016/j.geomorph.2022.108557,

Gehring E, Conedera M, Maringer J, Giadrossich F, Guastini E, Schwarz M (2019) Shallow landslide disposition in burnt European beech (Fagus sylvatica L.) forests. Sci Reports 9(1):1–11, https://doi.org/10.1038/s41598-019-45073-7

Hungr O, Jakob M (2005) Debris-flow hazards and related phenomena. Springer-Verlag, Berlin Heidelberg,. https://doi.org/10.1007/b138657

Hungr O, Leroueil S, Picarelli L (2014) The Varnes classification of landslide types, an update. Landslides 11(2):167–194. https://doi.org/10.1007/s10346-013-0436-y

Hürlimann M, Rickenmann D, Graf C (2003) Field and monitoring data of debris-flow events in the Swiss Alps. Canadian Geotech J 40(1):161–175. https://doi.org/10.1139/t02-087

Hürlimann M, Pinyol J, Moya J, Victoriano A, Génova M, Puig-polo C (2017) Recent debris flows in the Portainé catchment (Eastern Pyrenees , Spain): analysis of monitoring and field data focussing on the 2015 event. Landslides (September 2016):1161–1170, https://doi.org/10.1007/s10346-017-0832-9

Kean JW, McCoy SW, Tucker GE, Staley DM, Coe JA (2013) Runoff-generated debris flows: observations and modeling of surge initiation, magnitude, and frequency. J Geophys Res: Earth Surface 118(4):2190–2207
Key CH, Benson NC (2006) Landscape Assessment (LA) sampling and analysis methods. USDA Forest Service - General Technical Report RMRS-GTR (164 RMRS-GTR)
La Porta G, Leonardi A, Pirulli M, Cafaro F, Castelli F (2024) Time-resolved triggering and runout analysis of rainfall-induced shallow landslides. Acta Geotech 19(4):1873–1889. https://doi.org/10.1007/s11440-023-01996-0
Lei M, Cui Y, Ni J, Zhang G, Li Y, Wang H, Liu D, Yi S, Jin W, Zhou L (2022) Temporal evolution of the hydromechanical properties of soil-root systems in a forest fire in China. Sci Total Environ 809:151165, https://doi.org/10.1016/j.scitotenv.2021.151165,
Leonardi A, Pirulli M, Barbero M, Barpi F, Borri-Brunetto M, Pallara O, Scavia C, Segor V (2021) Impact of debris flows on filter barriers: analysis based on site monitoring data. Environment Eng Geosci 27(2):195–212. https://doi.org/10.2113/EEG-D-20-00013
Ma C, Deng J, Wang R (2018) Analysis of the triggering conditions and erosion of a runoff-triggered debris flow in Miyun County, Beijing. China Landslides 15(12):2475–2485. https://doi.org/10.1007/s10346-018-1080-3
Marchi L, Arattano M, Deganutti AM (2002) Ten years of debris-flow monitoring in the Moscardo Torrent (Italian Alps). Geomorphology 46(1–2):1–17. https://doi.org/10.1016/S0169-555X(01)00162-3
McCoy SW, Kean JW, Ja Coe, Staley DM, Ta Wasklewicz, Tucker GE (2010) Evolution of a natural debris flow: in situ measurements of flow dynamics, video imagery, and terrestrial laser scanning. Geology 38(8):735–738. https://doi.org/10.1130/G30928.1
Moody JA, Shakesby RA, Robichaud PR, Cannon SH, Martin DA (2013) Current research issues related to post-wildfire runoff and erosion processes. Earth-Sci Rev 122:10–37, https://doi.org/10.1016/j.earscirev.2013.03.004,
Morresi D, Marzano R, Lingua E, Motta R, Garbarino M (2022) Mapping burn severity in the western Italian Alps through phenologically coherent reflectance composites derived from Sentinel-2 imagery. Remote Sens Environment 269(November 2021):112800, https://doi.org/10.1016/j.rse.2021.112800,
Mueller R, Loew S (2009) Predisposition and cause of the catastrophic landslides of August 2005 in Brienz (Switzerland). Swiss Journal of Geosciences 102:331–344. https://doi.org/10.1007/s00015-009-1315-3
Pastor M, Quecedo M, González E, Herreros MI, Merodo JAF, Mira P (2004) Simple approximation to bottom friction for Bingham fluid depth integrated models. J Hydra Eng 130(2):149–155. https://doi.org/10.1061/(asce)0733-9429(2004)130:2(149)
Peduto D, Iervolino L, Foresta V (2022) Experimental analysis of the fire-induced effects on the physical, mechanical, and hydraulic properties of sloping pyroclastic soils. Geosci (Switzerland) 12(5), https://doi.org/10.3390/geosciences12050198
Pirulli M (2010) On the use of the calibration-based approach for debris-flow forward-analyses. Natural Hazards Earth Syst Sci 10(5):1009–1019. https://doi.org/10.5194/nhess-10-1009-2010
Pirulli M, Mangeney A (2008) Results of back-analysis of the propagation of rock avalanches as a function of the assumed rheology. Rock Mech Rock Eng 41(1):59–84. https://doi.org/10.1007/s00603-007-0143-x
Pirulli M, Pastor M (2012) Numerical study on the entrainment of bed material into rapid landslides. Geotechnique 62(11):959–972. https://doi.org/10.1680/geot.12.D.007
Pirulli M, Barbero M, Marchelli M, Scavia C (2017) The failure of the Stava Valley tailings dams (Northern Italy): numerical analysis of the flow dynamics and rheological properties. Geoenvironmental Disasters 4(1), https://doi.org/10.1186/s40677-016-0066-5,
Pirulli M, Leonardi A, Scavia C (2018) Comparison of depth-averaged and full-3D model for the benchmarking exercise on lanslide runout. Second JTC1 Workshop on Triggering and Propagation of Rapid Flow-like Landslides pp 1–14
Prochaska AB, Santi PM, Higgins JD, Cannon SH (2008) A study of methods to estimate debris flow velocity. Landslides 5(4):431–444. https://doi.org/10.1007/s10346-008-0137-0
Regione Piemonte (2018) Fenomeni dissestivi in Valle di Susa (TO) del Giugno 2018. Tech Rep
Regione Piemonte (2019) Piano straordinario di interventi di ripristino del territorio percorso dagli incendi boschivi dell'autunno 2017. Tech Rep
Rengers FK, McGuire LA, Kean JW, Staley DM, Dobre M, Robichaud PR, Swetnam T (2021) Movement of sediment through a burned landscape: sediment volume observations and model comparisons in the san gabriel mountains, california, usa. J Geophys Res: Earth Surface 126(7):e2020JF006053
Santi PM, Morandi L (2013) Comparison of debris-flow volumes from burned and unburned areas. Landslides 10(6):757–769. https://doi.org/10.1007/s10346-012-0354-4
Secci R, Calcina SV, Ranieri G, Uras G (2014) Analysis of the stability variation of a slope crossed by forest fire. Int J Civil Eng 3(1):41–50
Staley DM, Kean JW, Cannon SH, Schmidt KM, Laber JL (2013) Objective definition of rainfall intensity-duration thresholds for the initiation of post-fire debris flows in southern California. Landslides 10(5):547–562. https://doi.org/10.1007/s10346-012-0341-9
Stancanelli LM, Peres DJ, Cancelliere A, Foti E (2017) A combined triggering-propagation modeling approach for the assessment of rainfall induced debris flow susceptibility. J Hydro 550:130–143, https://doi.org/10.1016/j.jhydrol.2017.04.038,
Thomas MA, Rengers FK, Kean JW, McGuire LA, Staley DM, Barnhart KR, Ebel BA (2021) Postwildfire soil-hydraulic recovery and the persistence of debris flow hazards. J Geophys Res: Earth Surface 126(6):1–25. https://doi.org/10.1029/2021JF006091
Tiranti D, Cremonini R, Marco F, Gaeta AR, Barbero S (2014) The DEFENSE (debris Flows triggEred by storms - nowcasting system): an early warning system for torrential processes by radar storm tracking using a Geographic Information System (GIS). Comput Geosci 70:96–109, https://doi.org/10.1016/j.cageo.2014.05.004,
Tiranti D, Cremonini R, Asprea I, Marco F (2016) Driving factors for torrential mass-movements occurrence in the Western Alps. Frontier Earth Sci 4(February):1–13. https://doi.org/10.3389/feart.2016.00016
Tiranti D, Nicolò G, Gaeta AR (2019) Shallow landslides predisposing and triggering factors in developing a regional early warning system. Landslides 16(2):235–251. https://doi.org/10.1007/s10346-018-1096-8
Tiranti D, Cremonini R, Sanmartino D (2021) Wildfires effect on debris flow occurrence in Italian western alps: preliminary considerations to refine debris flow early warnings system criteria. Geosciences (Switzerland) 11(10), https://doi.org/10.3390/geosciences11100422
Vacha D (2021) Hydrologic and erosion response in burned watersheds (piedmont, western italian alps). PhD thesis
Vacha D, Mandrone G, Garbarino M, Morresi D (2021) First consideration about post 2017 wildfire erosion response and debris flow in Susa Valley (NW Italy). In: Understanding and Reducing Landslide Disaster Risk: Volume 4 Testing, Modeling and Risk Assessment 5th, pp 443–450
Vacha D, Mandrone G, Morresi D, Garbarino M (2022) Mapping post-fire monthly erosion rates at the catchment scale using empirical models implemented in GIS. A case study in Northern Italy. In: Progress in Landslide Research and Technology, vol 1, Springer
Venäläinen A, Korhonen N, Hyvärinen O, Koutsias N, Xystrakis F, Urbieta IR, Moreno JM (2014) Temporal variations and change in forest fire danger in Europe for 1960–2012. Natural Hazards Earth Syst Sci 14(6):1477–1490. https://doi.org/10.5194/nhess-14-1477-2014

G. La Porta (✉) · M. Pirulli
Department of Structural, Geotechnical and Building Engineering, Politecnico di Torino, Corso Duca degli Abruzzi, 24, 10129 Turin, Italy
Email: giulia.laporta@polito.it

M. Pirulli
Email: marina.pirulli@polito.it

A. Leonardi
Department of Civil and Structural Engineering, University of Sheffield, Mappin Street, S1 3JD Sheffield, UK
Email: a.leonardi@sheffield.ac.uk

S. La Ferlita
SRIA - Studio Rosso Ingegneri Associati Srl, Via Rosolino Pilo, 11, 10143 Turin, Italy
Email: laferlita@sria.it